Supporting Information

Efficient Ammonia Synthesis from Nitrate Reduction over Conjugated Nickel

Phthalocyanine Polymer under Wide Potential and Nitrate Concentration Range

Tahseen Ahmed,†[ab] Ling Zhang,†[a] Runzhi Wang,[ab] Yiling Bai,[c] Xuehua Zhang,*[a] Yu Sun,[ab] Lili Fu,[d] Bin Li,*[d] Menglei Yuan,[e] and Guangjin Zhang*[ab]

a. *CAS Key Laboratory of Green Process and Engineering, Institute of Process Engineering, Chinese Academy of Sciences, Beijing, 100190, China.*
b. *Center of Materials Science and Optoelectronics Engineering, Chinese Academy of Sciences, Beijing, 100049, China.*
c. *National Energy Center for Coal to Liquid, Synfuels China Technology Co., Ltd, Beijing, 101400, China.*
d. *Zhengzhou Tobacco Research Institute of CNTC, Zhengzhou, 450001, China*
e. *State Key Laboratory of Solidification Processing and School of Material Science and Engineering, North Western Polytechnical University, Xi'an, 710072, China*

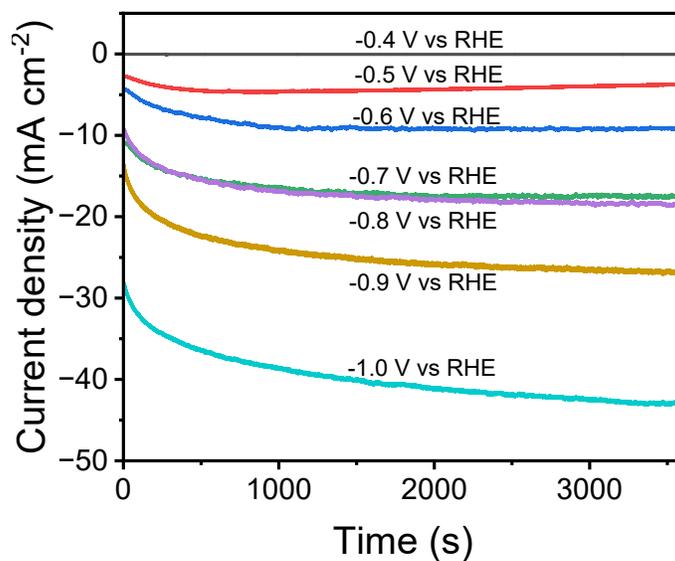*† Tahseen Ahmed and Ling Zhang contributed equally to this work.*

Fig. S1 I-t curves of NiPcP in 0.1 mol L^{-1} KNO$_3$ under different potentials.
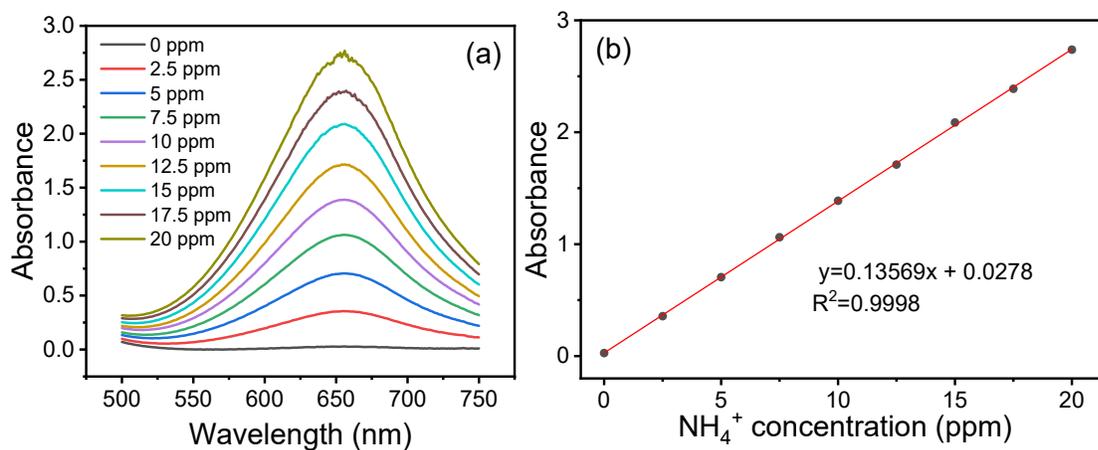

Fig. S2 (a) UV absorption spectra and (b) Standard curves of concentration-absorbance of standard NH$_4$Cl solution with different NH$_4^+$concentrations (0 – 20 µg mL^{-1}) in 0.1 M Na$_2$HPO$_4$. The absorbance at 655 nm was measured by UV-vis spectrophotometer. The standard curve shown good linear relation of absorbance with NH$_4$Cl concentration (y = 0.13569x + 0.0278, R^2 = 0.9998).
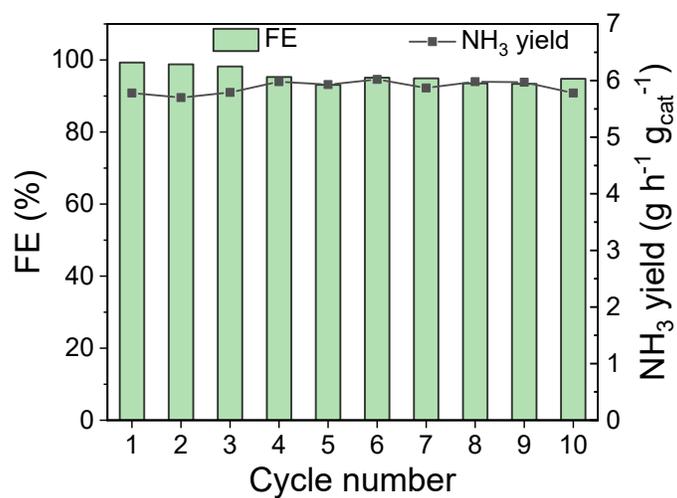
Fig. S3 The FE and NH$_3$ yield of NO$_3^-$RR based on NiPcP catalyst for 10 cycles at −0.7 V vs. RHE.
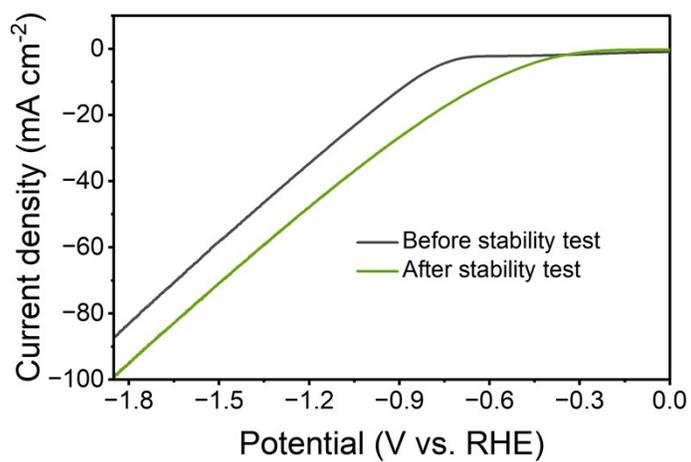

Fig. S4 The LSV curves of NiPcP in electrolyte containing NO$_3^-$ before and after stability testing.
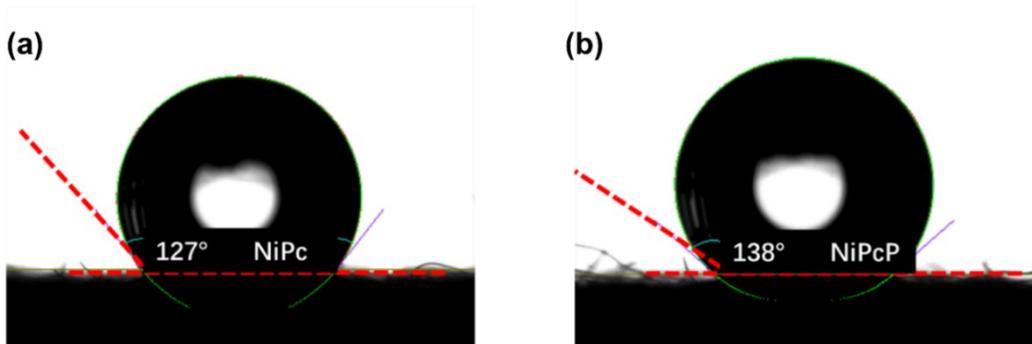
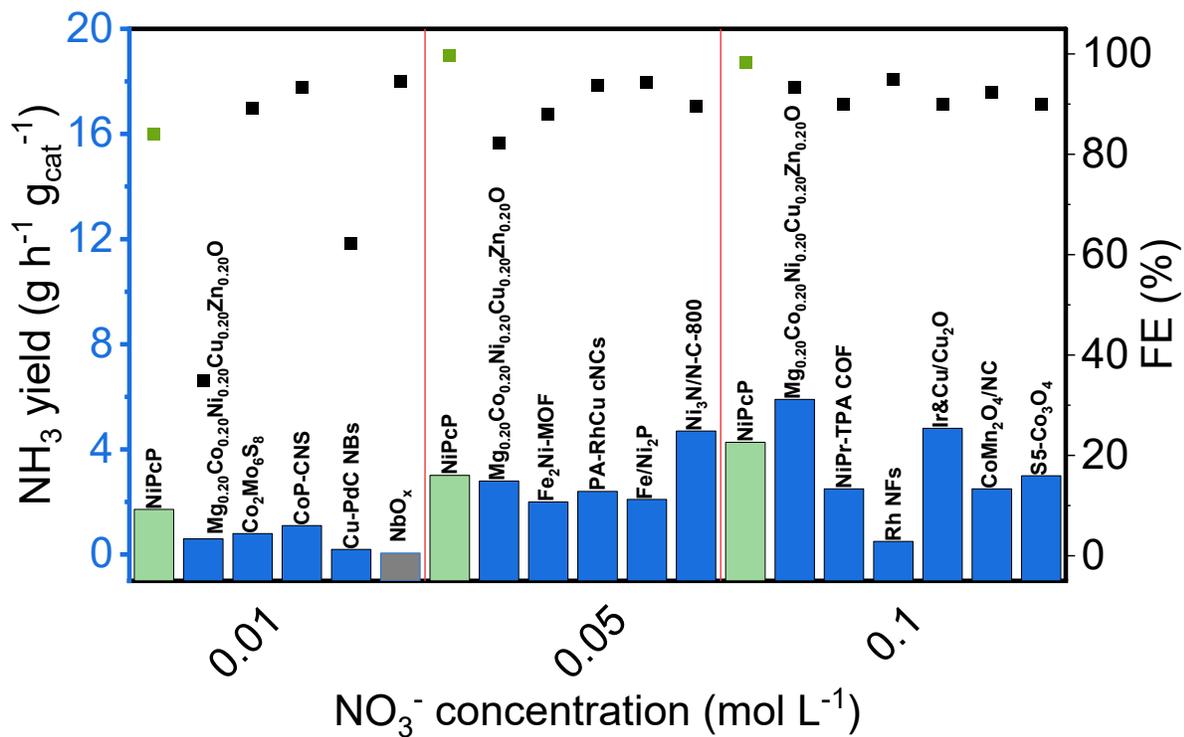**Fig. S5** The contact angle measurement of water on (a) NiPc and (b) NiPcP.

Fig. S6 A peer comparison of NO_3^-RR between the systems at different NO_3^- concentrations (0.01 mol L^{-1}, 0.05 mol L^{-1} and 0.1 mol L^{-1}, Ref. 16-29).

Table S1. Results of the corresponding control experiments for NO_3^-RR under -0.7 V vs. RHE within 2 h.

Parameters		FE (%)	NH_3 yield (g h^{-1} g$_{cat}^{-1}$)
NiPcP	KNO_3	99.7	3.01
NiPcP	-^{a}	0	0
-^{b}	KNO_3	42.1	0.19

^{a} Without KNO_3; ^{b} without catalyst, only carbon cloth as working electrode.

When KNO_3 was absent from the electrolyte, ammonia was not detected, ensuring that KNO_3 is the only N source for NH_3 product. If using pure carbon cloth as working electrode (without any catalyst), the FE and yield of ammonia were 42.1% and 0.19 g h^{-1} g$_{cat}^{-1}$, respectively. This is because carbon materials also exhibit weak catalytic activity for nitrate reduction, but the NH_3 yield (0.19 g h^{-1} g$_{cat}^{-1}$) is significantly lower than that of the NiPc (1.07 g h^{-1} g$_{cat}^{-1}$) or NiPcP (2.93 g h^{-1} g$_{cat}^{-1}$) catalysts under the same experimental conditions.

Table S2. FE and efficiency of NH_3 and by-products (nitrite, hydroxylamine, N_2 and H_2) in NO_3^-RR at -0.7 V vs. RHE within 2 h over NiPc and NiPcP.

Catalyst		NH_3	NO_2^-	NH_2OH	N_2	H_2
NiPcP	FE (%)	99.7	0.25	-	-	-
	Yield (g h^{-1} g$_{cat}^{-1}$)	3.01	-	-	-	-
NiPc	FE (%)	38.0	8.63	-	-	52.8
	Yield (g h^{-1} g$_{cat}^{-1}$)	0.56	1.31	-	-	3.03

Table S3 Comparison of NH_3 synthesis from NO_3^- reduction over NiPcP and other reported catalysts.

Electrocatalyst	Electrolyte	Potential	FE (%)	Yield	Ref.
NiPcP	0.05M KNO_3 + 0.1Na_2HPO_4	-0.7 V vs. RHE	99.7	3.01 g h^{-1} g^{-1}	This work
a-RuO_2	200 ppm NO_3^--N + 0.5 M Na_2SO_4	-0.35 V vs. RHE	96.42	0.1158 mmol h^{-1} cm^{-2}	[1]
Cu/Cu_2O NWAs	200 ppm NO_3^--N + 0.5 M Na_2SO_4	-0.85 V vs. RHE	95.52	0.2449 mmol h^{-1} cm^{-2}	[2]
TiO_2-x	50 ppm NO_3^--N + 0.5 M Na_2SO_4	-1.6 V vs. SCE	85	0.045 mmol h^{-1} mg^{-1}	[3]
Co_3O_4@NiO	200 ppm NO_3^--N + 0.5 M Na_2SO_4	-0.7 V vs. RHE	54.97	0.00693 mmol h^{-1} mg^{-1}	[4]
Fe SAC	0.5 M KNO_3 + 0.1 M K_2SO_4	-0.66 V vs. RHE	75	0.46 mmol h^{-1} cm^{-2}	[5]
Fe-PPy SACs	0.1 M KOH + 0.1 M KNO_3	-0.7 V vs. RHE	98.43	0.162 mmol h^{-1} cm^{-2}	[6]
Ni_{35}/NC-sd	0.5 M Na_2SO_4 + 0.3 M $NaNO_3$	-0.5 V vs. RHE	99	0.3 mmol h^{-1}cm^{-2}	[7]
OD-Ag	0.1 M KCl + 0.1 M NO_3^-	-1.35 V vs. Ag/AgCl	76.55	-	[8]
Pd/TiO_2	1 M LiCl + 0.25 M $LiNO_3$	-0.7 V vs. RHE	92.1	0.066 mmol h^{-1} cm^{-2}	[9]
Cu-incorporated	500 ppm NO_3^-	-0.4 V vs.	85.9	0.0256 mmol h^{-1}	[10]

PTCDA	+ 0.1 M PBS	RHE		cm^{-2}	
Pd (111)	0.1 M Na$_2$SO$_4$ + 0.1 M NO$_3^-$	-0.7 V vs. RHE	79.91	0.5485 mmol h^{-1} cm^{-2}	[11]
Cu@Th-BPYDC	1 M KOH + 0.1 M KNO$_3$	0 V vs. RHE	92.5	0.2253 mmol h^{-1} cm^{-2}	[12]
In-S-G	1 M KOH + 0.1 M KNO$_3$	-0.5 V vs. RHE	75	220 mmol h^{-1} g^{-1}	[13]
pCuO-5	0.05 M KNO$_3$ + 0.05 M H$_2$SO$_4$	-0.6 V vs. RHE	80	0.292 mmol h^{-1} cm^{-2}	[14]
Fluorine doped carbon	0.05 M H$_2$SO$_4$ + 200 ppm KNO$_3$	-0.65 V vs. RHE	20	23.8 mmol h^{-1} g^{-1}	[15]

Table S4 Comparison of NH$_3$ synthesis from NO$_3^-$ reduction over NiPcP and other reported catalysts at wide concentration range.

Catalyst	C$_{NO3-}$ (mM)	FE$_{NH3}$(%)	NH$_3$ Productivity (g h^{-1} g$_{cat}^{-1}$)	Ref.
NiPcP	10	84.1	1.7	This work
Mg$_{0.20}$Co$_{0.20}$Ni$_{0.20}$Cu$_{0.20}$Zn$_{0.20}$O	10	34.8	0.6	[16]
Co$_2$Mo$_6$S$_8$	10	89.2	0.8	[17]
CoP-CNS	10	93.3	1.1	[18]
Cu-PdC NBs	10	62.3	0.2	[19]
NbO$_x$	10	94.5	0.06	[20]
NiPcP	50	99.7	3.0	This work

$Mg_{0.20}Co_{0.20}Ni_{0.20}Cu_{0.20}Zn_{0.20}O$	50	82.2	2.8	[16]
Fe_2Ni-MOF	50	88.0	2.0	[21]
PA-RhCu cNCs	50	93.7	2.4	[22]
Fe/Ni_2P	50	94.3	2.1	[23]
Ni_3N/N-C-800	50	89.5	4.7	[24]
NiPcP	100	98.3	4.2	This work
$Mg_{0.20}Co_{0.20}Ni_{0.20}Cu_{0.20}Zn_{0.20}O$	100	93.4	5.9	[16]
NiPr-TPA COF	100	90.0	2.5	[25]
Rh NFs	100	95.0	0.5	[26]
$Ir\&Cu/Cu_2O$	100	90.0	4.8	[27]
$CoMn_2O_4/NC$	100	92.4	2.5	[28]
$S5$-Co_3O_4	100	89.9	3.0	[29]

References

1. Y. Wang, H. Li, W. Zhou, X. Zhang, B. Zhang and Y. Yu, Structurally Disordered RuO_2 nanosheets with rich oxygen vacancies for enhanced nitrate electroreduction to ammonia, *Angew Chem. Int. Ed.*, 2022, **61**, e202202604.
2. Y. Wang, W. Zhou, R. Jia, Y. Yu and B. Zhang, Unveiling the activity origin of a copper-based electrocatalyst for selective nitrate reduction to ammonia, *Angew Chem. Int. Ed.*, 2020, **59**, 5350-5354.

3. R. Jia, Y. Wang, C. Wang, Y. Ling and Y. Yu, Zhang B, Boosting selective nitrate electroreduction to ammonium by constructing oxygen vacancies in TiO_2, *ACS Catal.*, 2020, **10**, 3533-3540.
4. Y. Wang, C. Liu, B. Zhang and Y. Yu, Self-template synthesis of hierarchically structured Co_3O_4@NiO bifunctional electrodes for selective nitrate reduction and tetrahydroisoquinolines semi-dehydrogenation, *Sci. China Mater.*, 2020, **63**, 2530-2538.
5. Z. Y. Wu, M. Karamad, X. Yong, Q. Huang, D. A. Cullen, P. Zhu, C. Xia, Q. Xiao, M. Shakouri, F. Y. Chen, J. Y. Kim, Y. Xia, K. Heck, Y. Hu, M. S. Wong, Q. Li, I. Gates, S. Siahrostami and H. Wang, Electrochemical ammonia synthesis via nitrate reduction on Fe single atom catalyst, *Nat. Commun.*, 2021, **12**, 2870.
6. P. Li, Z. Jin, Z. Fang and G. Yu, A single-site iron catalyst with preoccupied active centers that achieves selective ammonia electrosynthesis from nitrate, *Energy Environ. Sci.*, 2021, **14**, 3522-3531.

7. P. Gao, Z. H. Xue, S. N. Zhang, D. Xu, G. Y. Zhai, Q. Y. Li, J. S. Chen and X. H. Li, Schottky barrier-induced surface electric field boosts universal reduction of NO_x^- in water to ammonia, *Angew Chem. Int. Ed.*, 2021, **60**, 20711-20716.

8. H. Liu, J. Park, Y. Chen, Y. Qiu, Y. Cheng, K. Srivastava, S. Gu, B. H. Shanks, L. T. Roling and W. Li, Electrocatalytic nitrate reduction on oxide-derived silver with tunable selectivity to nitrite and ammonia, *ACS Catal.*, 2021, **11**, 8431-8442.

9. Y. Guo, R. Zhang, S. Zhang, Y. Zhao, Q. Yang, Z. Huang, B. Dong and C. Zhi, Pd doping-weakened intermediate adsorption to promote electrocatalytic nitrate reduction on TiO_2 nanoarrays for ammonia production and energy supply with zinc–nitrate batteries, *Energy Environ. Sci.*, 2021, **14**, 3938-3944.

10. G. F. Chen, Y. Yuan, H. Jiang, S. Y. Ren, L. X. Ding, L. Ma, T. Wu, J. Lu and H. Wang, Electrochemical reduction of nitrate to ammonia via direct eight-electron transfer using a copper–molecular solid catalyst, *Nat. Energy*, 2020, **5**, 605-613.

11. Y. Han, X. Zhang, W. Cai, H. Zhao, Y. Zhang, Y. Sun, Z. Hu, S. Li, J. Lai and L. Wang, Facet-controlled palladium nanocrystalline for enhanced nitrate reduction towards ammonia, *J. Colloid Interface Sci*., 2021, **600**, 620-628.

12. Z. Gao, Y. Lai, Y. Tao, L. Xiao, L. Zhang and F. Luo, Constructing well-defined and robust Th-MOF-supported single-site copper for production and storage of ammonia from electroreduction of nitrate, *ACS Cent. Sci.*, 2021, **7**, 1066-1072.

13. F. Lei, W. Xu, J. Yu, K. Li, J. Xie, P. Hao, G. Cui and B. Tang, Electrochemical synthesis of ammonia by nitrate reduction on indium incorporated in sulfur doped graphene, *Chem Eng. J.*, 2021, **426**, 131317.

14. R. Daiyan, T. Tran-Phu, P. Kumar, K. Iputera, Z. Tong, J. Leverett, M. H. A. Khan, A. A. Esmailpour, A. Jalili, M. Lim, A. Tricoli, R. S. Liu, X. Lu, E. Lovell and R. Amal, Nitrate reduction to ammonium: from CuO defect engineering to waste NO_x-to-NH_3 economic feasibility, *Energy Environ. Sci.,* 2021, **14**, 3588-3598.

15. Y. Li, S. Xiao, X. Li, C. Chang, M. Xie, J. Xu and Z. Yang, A robust metal-free electrocatalyst for nitrate reduction reaction to synthesize ammonia, *Mater. Today Phys.*, 2021, **19**, 100431.

16. S. Sun, C. Dai, P. Zhao, S. Xi, Y. Ren, H. R. Tan, P. C. Lim, M. Lin, C. Diao, D. Zhang, C. Wu, A. Yu, J. C. J. Koh, W. Y. Lieu, D. H. L. Seng, L. Sun, Y. Li, T. L. Tan, J. Zhang, Z. J. Xu and Z. W. She, Spin-related Cu-Co pair to increase electrochemical ammonia generation on high-entropy oxides, *Nat. Commun.,* 2024, **15**, 260.

17. B. Li, F. Xia, Y. Liu, H. Tan, S. Gao, J. Kaelin, Y. Liu, K. Lu, T. J Marks and Y. Cheng, $Co_2Mo_6S_8$ catalyzes nearly exclusive electrochemical nitrate conversion to ammonia with enzyme-like activity, *Nano Lett.,* 2023, **23**, 1459-1466.

18. K. Fan, W. Xie, J. Li, Y. Sun, P. Xu, Y. Tang, Z. Li and M. Shao, Active hydrogen boosts electrochemical nitrate reduction to ammonia, *Nat. Commun.,* 2022, **13**, 7958.

19. Z. Wang, C. Sun, X. Bai, Z. Wang, X. Yu, X. Tong, Z. Wang, H. Zhang, H. Pang, L. Zhou, W. Wu, Y. Liang, A. Khosla and Z. Zhao, Facile synthesis of carbon nanobelts decorated with Cu and Pd for nitrate electroreduction to ammonia, *ACS Appl. Mater. Interfaces,* 2022, **14**, 30969−30978.

20. X. Wan, W. Guo, X. Dong, H. Wu, X. Sun, M. Chu, S. Han, J. Zhai, W. Xia, S. Jia, M. Hea and B. Han, Boosting nitrate electroreduction to ammonia on NbO_x via constructing oxygen vacancies, *Green Chem.,* 2022, **24**, 1090−1095.

21. Y. Lv, S. W. Ke, Y. Gu, B. Tian, L. Tang, P. Ran, Y. Zhao, J. Ma, J. L. Zuo and M. Ding, Highly efficient electrochemical nitrate reduction to ammonia in strong acid conditions with Fe_2M-trinuclear-cluster metal-organic frameworks, *Angew. Chem. Int. Ed.,* 2023, e202305246.

22. Z. X. Ge, T. J. Wang, Y. Ding, S. B. Yin, F. M. Li, P. Chen and Y. Chen, Interfacial engineering enhances the electroactivity of frame-like concave RhCu bimetallic nanocubes for nitrate reduction, *Adv. Energy Mater.,* 2022, **12**, 2103916.

23. R. Zhang, Y. Guo, S. Zhang, D. Chen, Y. Zhao, Z. Huang, L. Ma, P. Li, Q. Yang, G. Liang and C. Zhi, Efficient ammonia electrosynthesis and energy conversion through a Zn-nitrate battery by iron doping engineered nickel phosphide catalyst, *Adv. Energy Mater.,* 2022, **12**, 2103872.

24. X. Zhang, G. Ma, L. Shui, G. Zhou and X. Wang, Ni_3N nanoparticles on porous nitrogen-doped carbon nanorods for nitrate electroreduction, *Chem. Eng. J.,* 2022, **430**, 132666.

25. F. Lv, M. Sun, Y. Hu, J. Xu, W. Huang, N. Han, B. Huang and Y. Li, Near-unity electrochemical conversion of nitrate to ammonia on crystalline nickel porphyrin based covalent organic frameworks, *Energy Environ. Sci.,* 2023, **16**, 201–209.

26. H. Liu, J. Timoshenko, L. Bai, Q. Li, M. Rüscher, C. Sun, B. R. Cuenya and J. Luo, Low-coordination rhodium catalysts for an efficient electrochemical nitrate reduction to ammonia, *ACS Catal.,* 2023, **13**, 1513−1521.

27. M. A. Akram, B. Zhu, J. Cai, S. Qin, X. Hou, P. Jin, F. Wang, Y. He, X. Li and L. Feng, Hierarchical nanospheres with polycrystalline Ir&Cu and amorphous Cu_2O toward energy-efficient nitrate electrolysis to ammonia, *Small,* 2023, **19**, 2206966.

28. Z. Niu, S. Fan, X. Li, J. Duan and A. Chen, Interfacial engineering of $CoMn_2O_4$/NC induced electronic delocalization boosts electrocatalytic nitrogen oxyanions reduction to ammonia, *Appl. Catal. B Environ.,* 2023, **322**, 122090.

29. Z. Niu, S. Fan, X. Li, J. Yang, J. Wang, Y. Tao and G. Chen, Tailored electronic structure by sulfur filling oxygen vacancies boosts electrocatalytic nitrogen oxyanions reduction to ammonia, *Chem. Eng. J.,* 2023, **451**, 138890.